

Interfacing ab Initio Quantum Mechanical Method with Classical Drude Oscillator Polarizable Model for Molecular Dynamics Simulation of Chemical Reactions

Zhenyu Lu and Yingkai Zhang*

Department of Chemistry, New York University, New York 10003

Received April 5, 2008

Abstract: In order to further improve the accuracy and applicability of combined quantum mechanical/molecular mechanical (QM/MM) methods, we have interfaced the ab initio QM method with the classical Drude oscillator polarizable MM force field (ai-QM/MM-Drude). Different coupling approaches have been employed and compared: 1. the conventional dual self-consistent-field (SCF) procedure; 2. the direct SCF scheme, in which QM densities and MM Drude positions are converged simultaneously; 3. the microiterative SCF scheme, in which the Drude positions of the polarizable model are fully converged during each self-consistent field (SCF) step of QM calculations; 4. the one-step-Drude-update scheme, in which the MM Drude positions are updated only once instead of fully converged during each molecular dynamics (MD) step. The last three coupling approaches are found to be efficient and can achieve the desired convergence in a similar number of QM SCF steps comparing with the corresponding QM method coupled to a nonpolarizable force field. The feasibility and applicability of the implemented ai-QM/MM-Drude approach have been demonstrated by carrying out Born–Oppenheimer molecular dynamics simulations with the umbrella sampling method to determine potentials of mean force for both the methyl transfer reaction of the methyl chlorine-chlorine ion system and the glycine intramolecular proton transfer reaction in aqueous solution. Our results indicate that the ai-QM/MM-Drude approach is very promising, which provides a better description of QM/MM interactions while achieving quite similar computational efficiency in comparison with the corresponding conventional ab initio QM/MM method.

I. Introduction

The combined quantum mechanical/molecular mechanical (QM/MM) approaches^{1,2} have been widely used in modeling chemical reactions in complex systems, from the solid and surface catalysis to solution and enzyme reactions.^{3–12} With the increase of computer power and the development of more efficient algorithms which make high level electronic structure calculations more affordable, there is a great deal of interest in developing and applying QM/MM approaches based on ab initio quantum mechanical methods to achieve better accuracy and wider applicability. Over the past few years, this field is expanding rapidly, and molecular dynamics simulations with ab initio QM/MM methods have become

increasingly feasible.^{13–19} Meanwhile, it has been recognized that in order for ab initio QM/MM approaches to become an equal partner of experimental methods, significant development efforts are still needed.

In most QM/MM methods and applications, the conventional nonpolarizable molecular mechanical force fields have been employed, and QM/MM electrostatic interactions are calculated through a Coulombic term in an effective Hamiltonian with MM atoms as fixed point charges. In such a formulation, the electronic-configuration of the QM subsystem changes in response to the presence of MM electrostatic environment, while MM charges are always kept fixed. Thus it only takes into account the polarization effect of the MM charges on the QM subsystem but does not include the polarization effect of the QM subsystem on MM atoms or

* Corresponding author e-mail: yingkai.zhang@nyu.edu.

the polarization interactions among MM atoms. It is clear that the origin of this limitation comes from conventional pairwise additive force fields which use fixed atomic charges to model electrostatics. An intuitive and well-known step to make progress is to couple QM methods with polarizable MM force fields to achieve a consistent treatment of QM and MM electrostatic polarization interactions.^{20–41}

The available polarizable MM force fields can be mainly divided into three categories:^{42,43} the induced point dipole model,^{1,44–47} the fluctuating point charge model (also known as electronegativity equalization model),^{48–51} and the classical Drude oscillator model^{52–65} (also known as the shell model or charge-on-spring model). In the first two approaches, either atomic point dipoles or atomic charges are allowed to fluctuate in response to the environmental electric field changes. In the Drude oscillator model, an induced dipole is represented as a pair of point charges connected with a harmonic spring.

Among polarizable force fields, the induced dipole model was the first employed to interface with QM methods, which was presented when the QM/MM approach was introduced by Warshel and Levitt.¹ Later, the QM/induced-point-dipole method was further developed and implemented by a number of groups and had been employed to investigate the molecular properties in ground state and excited states and study the spectroscopy of organic molecules and biological systems.^{20–32} Instead of using the induced point dipole model, Bryce et al. and Field et al. used the fluctuating charge models in their QM/MM-pol calculations.^{33,34} Zhang et al. also made use of the fluctuating charge model to treat the polarizability of MM boundary atoms, and they demonstrated that including the mutual polarization of the QM and MM subsystems can yield more accurate results when modeling proton affinities.³⁷ Compared to the other two categories of polarizable models, the applications of the oscillator Drude model to the QM/MM calculations are seldom seen. Until very recently Geerke et al. combined semiempirical QM method with their charge-on-spring polarizable model (also known as the classical Drude oscillator model or shell model) to perform potential of mean force (PMF) simulations for a S_N2 reaction in the solvent dimethyl ether.³⁵ Besides the polarizable force field approaches, the importance of the mutual polarization between the QM and MM subsystems is also realized in QM/MM studies treating the environment with the reaction field approach.^{38–41}

Most of the above QM/MM-pol calculations so far employed a semiempirical Hamiltonian and a dual SCF procedure: at each iteration cycle, the MM induced dipoles/fluctuating charges were optimized in the presence of a frozen QM wave function, followed by the regular QM self-consistent field (SCF) calculation in the presence of external charges/dipoles. Generally, depending on the convergence criterion, two to five iterative cycles are usually needed to achieve the self-consistencies of both QM wave function and MM induced dipoles/fluctuating charges.^{20,23,35} Therefore, the dual SCF scheme makes the QM/MM-pol calculation significantly slower than the corresponding conventional QM/MM calculation. This is especially problematic for the ab initio QM/MM-pol approach, in which the QM SCF calculation

is much more expensive than the one in semiempirical QM methods. To circumvent the dual SCF scheme and improve the computational efficiency, Dupuis et al. presented a direct SCF approach,²⁶ in which QM wave functions and MM induced dipoles are converged simultaneously instead of iteratively. With this direct SCF algorithm, they studied the structure and energy of the formaldehyde and water complex in the ground state and excited state with ai-QM/MM-pol calculations.²⁶

From the above account, it is very clear that to couple QM methods with polarizable force fields is both desirable and feasible. However, the QM/MM-pol approaches have been rarely adopted in QM/MM studies of chemical reactions so far, even with the recent renewed enthusiasm in the development of polarizable force fields. Besides the availability of polarizable force field parameters, the lack of popularity of the QM/MM-pol approaches may also be due to the following two concerns: one is the computational cost of such calculations, and the other is the effect of such consistent treatment of polarization on the final results. It can be easily envisioned that the QM/MM-pol approaches would meet much less resistance if they can be demonstrated to have a similar efficiency while better accuracy than the corresponding conventional QM/MM methods. Thus in this paper, we have interfaced ab initio QM methods with the classical Drude oscillator polarizable MM force field (ai-QM/MM-Drude) for Born-Oppenheimer molecular dynamics simulations of chemical reactions. In order to improve the efficiency and stability of such simulations, we have explored several schemes of optimizing/updating the Drude particles during MD simulations. The resulted ai-QM/MM-Drude methods have been tested on the water dimer and applied to calculate the potentials of mean force for both the methyl transfer reaction of the methyl chlorine-chlorine ion system and the glycine intramolecular proton transfer reaction in aqueous phase. The results and computational efficiency have been compared with the corresponding conventional ai-QM/MM methods. Our work indicates that the ai-QM/MM-Drude approach is very promising, which provides a more realistic description of QM/MM interactions while achieving quite similar computational efficiency in comparison with the corresponding conventional ai-QM/MM method. We also found that the inclusion of polarization effects can have a significant effect on the calculated free energy profile for the glycine intramolecular proton transfer reaction in aqueous solution.

The outline of the paper is as follows: In section II we give a brief introduction to the Drude oscillator model and the conventional QM/MM approach, followed by the description about the coupling between the QM Hamiltonian and the Drude oscillator model, and the one-step-Drude-update scheme for QM/MM-Drude MD simulations. In section III we present the computational details. Results and discussion are given in section IV.

II. Methodology

A. Classical Drude Oscillator Model. In the classical Drude oscillator model, the induced dipole is represented

by a pair of point charges separated by a variable distance. One point charge q_α is fixed to the charge center site while the other point charge (called Drude particle) $q_{\alpha'}$ is bounded to the charge center site via a harmonic spring of force constant $k_{\alpha'}$. The net charge and dipole moment on this charge center site are $q_\alpha + q_{\alpha'}$ and $\mu_{\alpha'} = q_{\alpha'} \mathbf{d}_{\alpha'}$, where $\mathbf{d}_{\alpha'} = |\mathbf{r}_{\alpha'} - \mathbf{r}_\alpha|$. The total electrostatic energy of the system for a Drude oscillator system is

$$E_{ele} = E_{static-ele} + E_{Drude-ele} + E_{self} \\ = \sum_{\alpha} \sum_{\beta > \alpha} \frac{q_{\alpha} q_{\beta}}{r_{\alpha\beta}} + \left(\sum_{\alpha} \sum_{\beta'} \frac{q_{\alpha} q_{\beta'}}{r_{\alpha\beta'}} + \sum_{\alpha'} \sum_{\beta' > \alpha'} \frac{q_{\alpha'} q_{\beta'}}{r_{\alpha'\beta'}} \right) + \frac{1}{2} \sum_{\alpha'} k_{\alpha'} d_{\alpha'}^2 \quad (2.1)$$

where the prime denotes the Drude particle site. Comparing the self-energy term in the above equation with the one from the induced dipole model

$$E_{self} = \frac{1}{2} \sum_{\alpha'} \frac{\mu_{\alpha'}^2}{\alpha_{\alpha'}}$$

it leads to the following expression for the isotropic atomic polarizability

$$\alpha_{\alpha'} = \frac{q_{\alpha'}^2}{k_{\alpha'}} \quad (2.2)$$

B. QM/MM Approach. The total energy of a QM/MM system can be written as

$$E_{tot} = E_{qm} + E_{qm/mm} + E_{mm} \quad (2.3)$$

For the Hartree-Fock theory or the Kohn–Sham density functional theory, E_{qm} can be written as

$$E_{qm} = \sum_{\mu\nu}^{AO} D_{\mu\nu} H_{\mu\nu}^{core} + \frac{1}{2} \sum_{\mu\nu\lambda\sigma}^{AO} D_{\mu\nu} D_{\lambda\sigma} (\mu\nu\lambda\sigma) + E^{XC}[\rho] \quad (2.4)$$

where μ, ν denote the atomic basis set, $D_{\mu\nu}$ is the density matrix element, and $E^{XC}[\rho]$ is the exchange-correlation functional of electron density whose form depends on the theory used. $E_{qm/mm}$ is the coupling term between the QM and MM subsystem and can be decomposed into

$$E_{qm/mm} = E_{qm/mm}^{ele} + E_{qm/mm}^{vdw} + E_{qm/mm}^{MM-bonded} \quad (2.5)$$

where $E_{qm/mm}^{MM-bonded}$ refers to the bond, angle, and dihedral energy terms at the QM/MM interface. In the actual implementation, the QM/MM electrostatic coupling enters into the QM SCF calculation by adding the following one-electron core Hamiltonian into the Fock matrix $F_{\mu\nu}$

$$H_{\mu\nu}^{core, qm/mm} = \langle \mu | - \sum_i \sum_{\alpha} \frac{q_{\alpha}}{r_{i\alpha}} | \nu \rangle \quad (2.6)$$

where q_{α} is the MM atomic charge, and i is the index for electron. Then

$$E_{qm/mm}^{ele} = \sum_{\mu, \nu}^{AO} D_{\mu\nu} H_{\mu\nu}^{core, qm/mm} + \sum_A^{QM} \sum_{\alpha}^{MM} \frac{Q_A q_{\alpha}}{r_{A\alpha}} \quad (2.7)$$

where Q_A is the QM nuclei charge. Now combining eqs 2.4 and 2.7, the final electronic energy can be obtained after determining $D_{\mu\nu}$ with the SCF approach according to the variational principle.

C. QM/MM-Drude Oscillator Model. In the QM/MM-Drude approach, the total energy of the system can be written as

$$E_{tot} = E_{qm} + E_{qm/mm} + E_{mm} + E_{Drude-ele} + E_{self} \quad (2.8)$$

where $E_{Drude-ele}$ is the electrostatic energy term involving the Drude particles

$$E_{Drude-ele} = \sum_{\alpha}^{MM} \sum_{\beta'}^{MM'} \frac{q_{\alpha} q_{\beta'}}{r_{\alpha\beta'}} + \sum_{\alpha'}^{MM'} \sum_{\beta' > \alpha'}^{MM'} \frac{q_{\alpha'} q_{\beta'}}{r_{\alpha'\beta'}} + \sum_A^{QM} \sum_{\alpha}^{MM'} \frac{Q_A q_{\alpha}}{r_{A\alpha'}} + \sum_{\mu, \nu}^{AO} D_{\mu\nu} \langle \mu | - \sum_i^{electron} \sum_{\alpha'}^{MM'} \frac{q_{\alpha'}}{r_{i\alpha'}} | \nu \rangle \\ = \sum_{\alpha'}^{MM'} q_{\alpha'} \left(\varphi_{\alpha'}^{MM} + \frac{1}{2} \varphi_{\alpha'}^{MM'} + \varphi_{\alpha'}^{Nuc} + \varphi_{\alpha'}^{electron} \right) \quad (2.9)$$

and

$$E_{self} = \frac{1}{2} \sum_{\alpha'}^{MM'} k_{\alpha'} d_{\alpha'}^2 \quad (2.10)$$

Here $\varphi_{\alpha'}^{MM}$, $\varphi_{\alpha'}^{MM'}$, $\varphi_{\alpha'}^{Nuc}$, $\varphi_{\alpha'}^{electron}$ are the electrostatic potentials at the Drude site α' generated by the classical point charges (whose positions are immobile during the energy evaluation), the charges of Drude particles, the QM nuclei charge, and QM wave function, respectively. Again the prime indicates the Drude particle site.

It is clear from eqs 2.4, 2.7, 2.9, and 2.10 that now the total energy of the system should be minimized with respect to both $D_{\mu\nu}$ and the Drude particle position $\mathbf{r}_{\alpha'}$. Typically, a dual SCF coupling procedure can be employed:

(1) With a frozen QM density, according to eqs 2.9 and 2.10 the Drude particle positions are updated to satisfy

$$\nabla_{\mathbf{r}_{\alpha'}} \left(E_{Drude-ele} + E_{self} \right) = - \sum_{\alpha'}^{MM'} q_{\alpha'} \left(\mathbf{E}_{\alpha'}^{MM} + \frac{1}{2} \mathbf{E}_{\alpha'}^{MM'} + \mathbf{E}_{\alpha'}^{Nuc} + \mathbf{E}_{\alpha'}^{electron} \right) + k_{\alpha'} \mathbf{d}_{\alpha'} = 0 \quad (2.11)$$

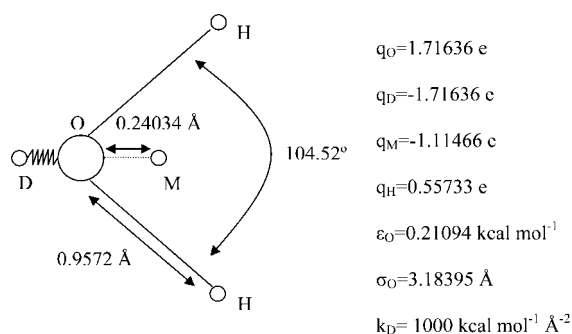
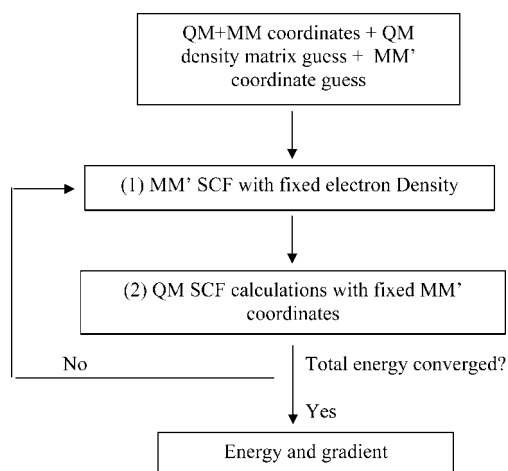
or rearranged as

$$\mathbf{d}_{\alpha'} = \frac{1}{k_{\alpha'}} \sum_{\alpha'}^{MM'} q_{\alpha'} \left(\mathbf{E}_{\alpha'}^{MM} + \frac{1}{2} \mathbf{E}_{\alpha'}^{MM'} + \mathbf{E}_{\alpha'}^{Nuc} + \mathbf{E}_{\alpha'}^{electron} \right) \quad (2.12)$$

Either a SCF approach based on eq 2.12 (since the electric field $\mathbf{E}_{\alpha'}$ depends on $\mathbf{d}_{\alpha'}$) or a minimization method based on eq 2.11 can be applied to obtain $\mathbf{d}_{\alpha'}$ or equivalently $\mathbf{r}_{\alpha'}$.

(2) With the updated Drude particle positions determined from step (1), regular QM SCF calculations as implemented in QM software packages are performed to obtain a converged $D_{\mu\nu}$. If the total energy is converged, exit; otherwise, go back to step (1).

For clarity, the above dual SCF coupling procedure is illustrated in Scheme 2, which has been employed in most QM/MM-pol methods.

Scheme 1. Parameters of the SWM4-NDP Water Model^{64,65}**Scheme 2.** Dual SCF Scheme for QM/MM-Drude Calculations

D. Direct SCF and Microiterative SCF Coupling Schemes. Although the dual SCF coupling is very straightforward to implement, it increases QM SCF steps and makes QM/MM-pol calculations significantly slower than the corresponding conventional QM/MM calculations. The alternative is the direct SCF coupling scheme presented by Dupuis et al.,²⁶ in which step (1) and step (2) are combined so that the QM wave function and the MM induced dipoles can be converged simultaneously. In our current work, we extend the direct SCF algorithm to treat the coupling between the Drude oscillators and the QM wave function, and the details are described as follows:

(A) At each QM SCF step, the current density matrix is used to update the Drude particle positions only once according to eq 2.12.

(B) The one-electron integral

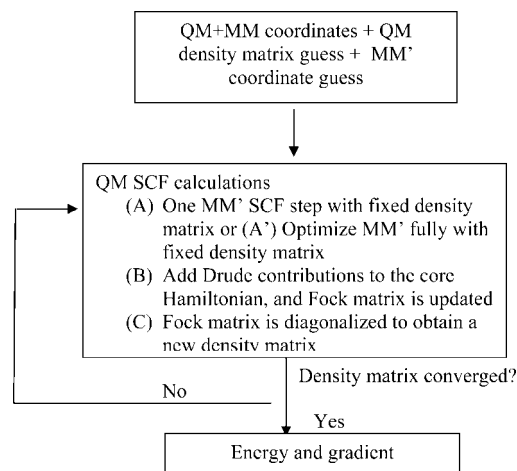
$$\langle \mu | - \sum_i^{electron} \sum_{\alpha'}^{MM'} \frac{q_{\alpha'}}{r_{i\alpha'}} | \nu \rangle$$

is calculated and added to the core Hamiltonian;

(C) The updated Fock matrix is diagonalized to obtain a new density matrix. If the density matrix and the total energy are converged, exit; otherwise start another QM SCF step.

If we replace the step (A) with a fully optimization step (A'):

(A') At each QM SCF step, the current density matrix is used to fully optimize the Drude particle positions according to eq 2.12.

Scheme 3. Direct and Microiterative SCF Schemes for QM/MM-Drude Calculations

We obtain a microiterative SCF coupling scheme. From the above description, we can see that step (1) in the dual SCF algorithm corresponds to step (A'), a microiteration step as part of the QM SCF step. In the direct SCF and microiterative coupling schemes, due to the re-evaluations of the one-electron integral

$$\langle \mu | - \sum_i^{electron} \sum_{\alpha'}^{MM'} \frac{q_{\alpha'}}{r_{i\alpha'}} | \nu \rangle$$

at each QM SCF step, the core Hamiltonian keeps changing until convergence. For clarity, the direct SCF and microiterative SCF coupling schemes are illustrated in Scheme 3.

Compared to the conventional QM/MM approach, the increase of computational time in the QM/MM-Drude calculation using the direct SCF algorithm or the microiterative SCF coupling scheme may also come from the following two aspects:

(1) Computing $\mathbf{E}_{\alpha'}$ according to eq 2.12 for updating the Drude particle positions at step (A) or (A') and evaluating

$$\langle \mu | - \sum_i^{electron} \sum_{\alpha'}^{MM'} \frac{q_{\alpha'}}{r_{i\alpha'}} | \nu \rangle$$

at step (B).

(2) The possible increase of QM SCF steps in comparison to the conventional QM/MM calculation.

For the second concern, as demonstrated later from our tests, there is almost no increase of QM SCF steps in our ai-QM/MM-Drude MD simulations. The cost due to (1) needs some comments. Although the two-electron coulomb integral and exchange-correlation integral calculations are computationally much more expensive than the one-electron integral and MM calculations, the cost of computing $\mathbf{E}_{\alpha'}$ and one-electron integrals repetitively involving the Drude particles is still not ignorable, especially when the size of MM-Drude system is large. If $\mathbf{d}_{\alpha'}$ remains small enough (which means the current Drude oscillator model is a good approximation to the induced point dipole model), then $\mathbf{E}_{\alpha'}$ can be well approximated by \mathbf{E}_{α} , the electric field at the fixed charge center site. Unlike $\mathbf{E}_{\alpha'}$ which is dependent on the position of the mobile Drude particles, \mathbf{E}_{α} needs to be

computed only once at each QM SCF step. The work from Thompson²¹ indicates that for $d_{\alpha'} < 0.1 \text{ \AA}$, the error in energy caused by such an approximation is small. This approximation was taken by Geerke et al. in their semiempirical QM/MM-Drude MD simulations.³⁵ However, it has been very recently found that the resulted error can be quite significant unless the charges of Drude particles are very large.⁶⁶ Here we did not take such an approximation and evaluated $\mathbf{E}_{\alpha'}^{\text{electron}}$ whenever the Drude particles move. Therefore, the microiterative SCF coupling scheme is more computationally demanding than the direct SCF scheme, because of the repetitive $\mathbf{E}_{\alpha'}$ calculations at each QM step in the former approach.

E. One-Step-Drude-Update Scheme. In MD simulations with polarizable force fields, instead of obtaining the converged $\mathbf{d}_{\alpha'}$ with either an optimizer or a SCF approach, there are two more efficient ways for updating the Drude particle positions at each MD step. One is called the extended Lagrangian method,⁶⁷ in which the Drude particles are assigned with a fictitious mass and treated as dynamic variables and their positions are propagated according to the extended Lagrangian function. By coupling the motions of the Drude particles with a low-temperature thermostat, the system can remain close to the SCF regime.⁶⁸ Another method to avoid the SCF calculations in MD polarizable force field simulations is called the always stable predictor-corrector (ASPC) method.^{69,70} In this method, the induced dipoles (or $\mathbf{d}_{\alpha'}$ for Drude oscillator model) at time $t+h$ is

$$\boldsymbol{\mu}(t+h) = \omega M(\boldsymbol{\mu}^p(t+h)) + (1-\omega)\boldsymbol{\mu}^p(t+h) \quad (2.13)$$

where h denotes the time step, ω is the relaxation parameter to ensure the stability, which prevents the error in $\boldsymbol{\mu}(t+h)$ accumulating along the trajectory, and M represents the right-hand side (RHS) equation for $\boldsymbol{\mu}$ in the SCF procedure. From eq 2.12 we can see that the RHS equation of $\mathbf{d}_{\alpha'}$ in the Drude oscillator model is just

$$M \equiv \frac{1}{k_{\alpha'}} \sum_{\alpha'}^{MM'} q_{\alpha'} \left(\mathbf{E}_{\alpha'}^{MM} + \frac{1}{2} \mathbf{E}_{\alpha'}^{MM'} + \mathbf{E}_{\alpha'}^{\text{Nuc}} + \mathbf{E}_{\alpha'}^{\text{electron}} \right) \quad (2.14)$$

In eq 2.13, $\boldsymbol{\mu}^p(t+h)$ is the guess of the induced dipole based on the historical information from previous MD steps. While the simplest form is just a linear extrapolation, $\boldsymbol{\mu}^p(t+h) = 2\boldsymbol{\mu}(t) - \boldsymbol{\mu}(t-h)$, Kolafa gave more elaborate forms to improve the accuracy and time reversibility.^{69,70}

Recently Niklasson et al. proposed a lossless time-reversible ab initio QM MD scheme,^{71,72} which allows stable Hatree-Fock MD simulations with only one single QM SCF cycle per time step. In our current work, we extend their method to update the positions of Drude particles in a similar manner as they update the density matrix along the MD simulations. Specifically

$$\mathbf{d}_{\alpha'}^p(t+h) = 2\mathbf{d}_{\alpha'}(t) - \mathbf{d}_{\alpha'}^p(t-h) \quad (2.15)$$

$$\mathbf{d}_{\alpha'}(t+h) = M(\mathbf{d}_{\alpha'}^p(t+h)) \quad (2.16)$$

where M is defined in eq 2.14. In eq 2.15 a simple linear extrapolation form is used, and the time reversibility is

reserved by using $\mathbf{d}_{\alpha'}^p(t-h)$ instead of $\mathbf{d}_{\alpha'}(t-h)$. As tested, the resulted lossless time-reversible MD with one-step-Drude-update scheme allows a stable MM Drude oscillator MD simulation by updating the positions of Drude particles only once at each time step. The details of integrating this lossless time-reversible MD scheme into QM/MM-Drude MD simulations are described in Scheme 4.

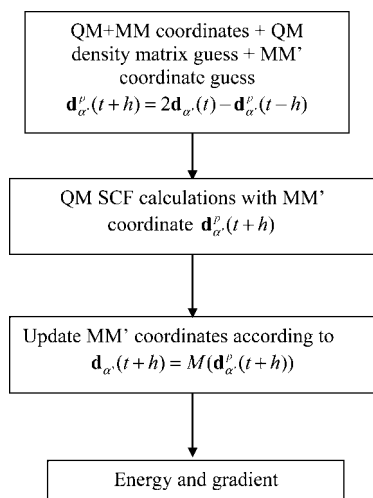
III. Computational Details

In the QM/MM-Drude oscillator approach, for the water solvent, we employed a SWM4-NDP model, a Drude oscillator model from Lamoureux et al.,^{64,65} which is calibrated to reproduce important bulk properties of the water at room temperature and pressure. The parameters of the SWM4-NDP water model are shown in Scheme 1. In conventional QM/MM calculations, we use the TIP3P water model.⁷³ The QM/MM and QM/MM-Drude schemes were implemented by modifying Gaussian03⁷⁴ and the TINKER program.⁷⁵ The correctness of the implementation has been carefully checked by comparing the analytical and numerical gradients and the energy conservation from short NVE MD runs.

For the PMF calculation of glycine intramolecular proton transfer reaction, the solutes were solvated with a 20 Å sphere of waters. Only the waters within 15 Å of the sphere center were allowed to move during the MD simulations. For the methyl-transfer reaction, the solute was solvated with a 18 Å sphere of waters, and only 13 Å of the sphere center were allowed to move during MD simulations. The bonds in water molecules were constrained using the RATTLE algorithm.^{76,77} A time step of 1 fs was employed for the MD simulations, and the mass of deuterium was used for the hydrogen atoms in the glycine molecule. No cutoff was used for the nonbonded interactions. The velocity verlet integrator implemented in the TINKER program was used, and the temperatures of the systems were controlled at 300 K with the Berendsen velocity scaling method.⁷⁸ The PMF calculations were performed with the umbrella sampling and the Weighted Histogram Analysis method.^{79,80}

For the methyl transfer reaction of the methyl chlorine-chlorine ion system, the reaction coordinate (rc) is chosen as $rc = d_{c-cl1} - d_{c-cl2}$, and 22 windows centering from reaction coordinate of -3.8 to 0.0 \AA were used. The symmetry was used to obtain a full PMF curve. For each window, 10 ps equilibration was performed, followed by a 20 ps data collection. HF/6-31G(d) was employed for the QM calculations. The convergence criterion in the microiterative SCF algorithm was set to rms gradient $0.001 \text{ kcal mol}^{-1} \text{ \AA}^{-2}$ per Drude.

For the glycine intramolecular proton transfer reaction, the reaction coordinate is defined as $rc = d_{H10-N1} - d_{H10-O5}$ (see Figure 1), and 17 windows were employed. For each window, 12 ps equilibration were performed, followed by 24 ps data collection. B3LYP/6-31G(d) was employed for the QM calculations. The convergence criterion in the microiterative SCF algorithm was set to rms gradient $0.01 \text{ kcal mol}^{-1} \text{ \AA}^{-2}$ per Drude. The Lennard-Jones parameters from the Amber94 force field⁸¹ were used for the QM subsystems in both ai-QM/MM-Drude and ai-QM/MM

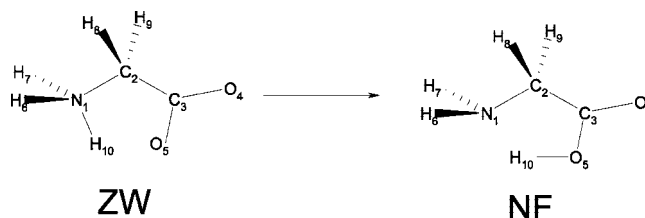
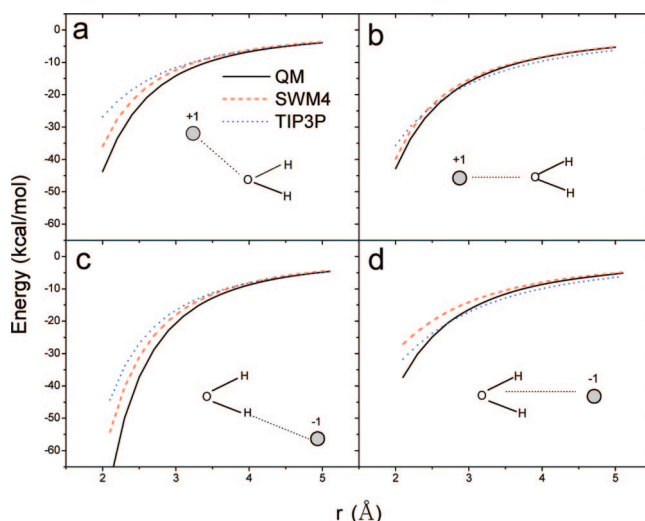
Scheme 4. One-Step-Drude-Update Scheme for QM/MM-Drude MD Simulations

calculations. It should be noted that ideally different QM van der Waals parameters should be used to further improve the description of QM/MM interactions. Some work was already done in parametrizing the QM van der Waals parameters for the QM/MM models,^{82–84} but the influence of the QM van der Waals parameters on the ai-QM/MM-Drude calculations has not been addressed. The work along this direction is currently in progress and will be presented in future publications.

IV. Results and Discussion

A. Comparison between the SWM4-NDP Water and the QM Water. As illustrated in Scheme 1, the SWM4-NDP water model^{64,65} uses the point charges for electrostatic interactions and the 12–6 Lennard-Jones potentials for the repulsive and dispersion interactions. The molecular polarizability is modeled by a Drude particle attached to the oxygen atom. According to eq 2.2, the molecular polarizability given by this model is 0.97825 \AA^3 , much smaller than the experimental value 1.44 \AA^3 . The reduced molecular polarizability was found to be essential in reproducing the liquid properties,⁶⁴ which may be due to the simplicity of this model.

Before applying this water model in our ai-QM/MM-Drude simulations, it will be informative to learn how accurate this simple polarizable water model is in modeling the electrostatic interactions. To avoid the complexity caused by choosing Lennard-Jones parameters, we studied the interactions between a water and a point charge. As shown in the insets of Figure 2, we moved either a +1e or –1e point charge in four different directions and calculated the interaction energies along the charge-oxygen distance for the SWM4-NDP water, the TIP3P water, and the QM water in the MP2/aug-cc-pvtz description. From Figure 2 we can see that in general the SWM4-NDP water model yields a better agreement with the QM description than the TIP3P water, although the electrostatic interactions are underestimated in the SWM4-NDP water, which is not a surprise considering that the molecular polarizability given by SWM4-NDP is

**Figure 1.** Glycine intramolecular proton transfer reaction.**Figure 2.** Electrostatic interaction energies between a water and a point charge as a function of charge-oxygen distance. The insets illustrate the approaching directions of the point charge (+1 or –1): (a) along the oxygen electron lone pair direction; (b) along the C₂ axis of the symmetry; (c) along the O–H bond direction; and (d) along the C₂ axis of the symmetry from the side of the hydrogen atoms.

significantly lower than the values from experiments or the MP2/aug-cc-pvtz calculation.

Another test we performed is to calculate the water dimer interaction energies. The QM calculations were done at the B3LYP/6–31G(d,p) level. Two cases were considered for the QM/MM-Drude and QM/MM calculations. One corresponds to the QM water as the hydrogen bond donor, while in the other case the QM water is the hydrogen bond acceptor. For the QM/MM-Drude calculations, the Lennard-Jones parameters of the QM water are taken from those of the SWM4-NDP water model, while in the QM/MM calculations, the Lennard-Jones parameters of the QM water are taken from those of the TIP3P water model. As illustrated in Figure 3, in contrary to those from the QM/MM calculations, the QM/MM-Drude calculations for the two cases considered yield the consistent binding energies and binding distances and have close agreement with those from pure QM calculations, which suggest that the SWM4-NDP water has a better performance in terms of “mimicking” the QM water than the TIP3P water does. These results are encouraging, which indicate that the ai-QM/MM-Drude method can provide a better description of QM/MM interactions than the corresponding conventional ai-QM/MM method.

B. Computational Efficiency of ai-QM/MM-Drude MD Simulations. To evaluate the feasibility of ai-QM/MM-Drude calculations, we performed short-time MD simulations for several systems with both conventional ai-QM/MM and

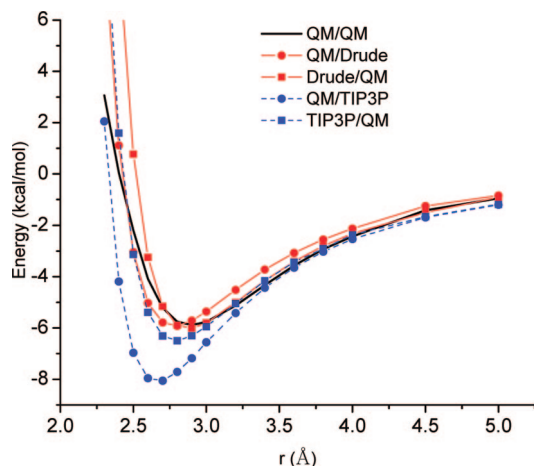


Figure 3. Water dimer interaction energies as a function of the O–O distance. QM–QM denotes QM treatment for the whole water dimer; QM–SWM4 (TIP3P) denotes QM for the acceptor and SWM4–NDP (TIP3P) for the donor; and SWM4 (TIP3P)–QM denotes QM for the donor and SWM4–NDP (TIP3P) for the acceptor.

ai-QM/MM-Drude simulations. The computational efficiency of the dual SCF, direct SCF, and microiterative SCF schemes as well as the one-step-Drude-update scheme have been tested. The results of these short MD simulations (0.1 ps \sim 1.0 ps) are summarized in Table 1. First we observe that in comparison with conventional QM/MM calculations, except the dual SCF scheme, coupling the QM subsystem with the MM-Drude subsystem will not increase the QM SCF steps for all the other three Drude optimization/updating schemes. Second, among the different Drude optimization/updating schemes, the one-step-Drude-update scheme is the most efficient one. This is fully expected because comparing with other schemes, there is no increase in the QM SCF steps and no repetitive one-electron integrals calculation involved in this scheme. Third, the increase in the size of the QM subsystem leads to the decrease of the time ratio between ai-QM/MM MD and ai-QM/MM-Drude MD, which becomes more close to the unity. We can see that for a medium QM subsystem of \sim 300 basis functions, the increase of computational time due to employing the Drude oscillator polarizable force field becomes insignificant for the direct SCF, microiterative SCF, and one-step-Drude-update schemes.

C. Potential of Mean Force Calculations of the Chemical Reactions in Solution. The chemical reactions often involve the charge transfer steps, which cause significant changes of the electrostatic properties around the reaction center. The polarizable waters should be able to adapt to the change of electronic configurations of the reaction center by adjusting its dipole moments, which in turn has an impact on the charge distributions of the reaction center. Therefore, the polarizable water model may have a strong influence on the calculated energetics of chemical reactions. In this work, we have investigated two chemical reactions in solution, one is a S_N2 reaction, the methyl transfer of the methyl-chlorine-chlorine ion system, and the other is the glycine intramolecular proton transfer reaction (see Figure 1).

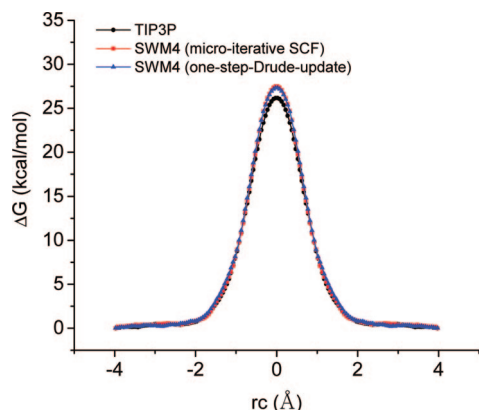
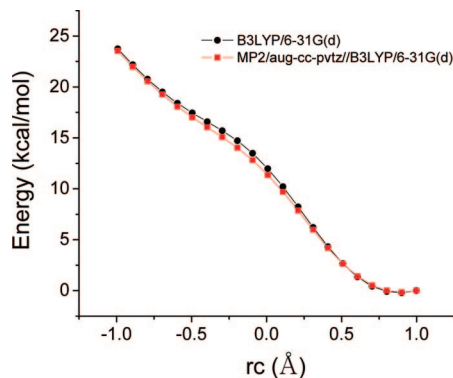
The potential of mean force curves for the S_N2 reaction is shown in Figure 4. We obtained a barrier of 26.2 kcal/mol from the HF(6–31G(d))/TIP3P simulation and 27.5 kcal/mol from the HF(6–31G(d))/SWM4–NDP simulation. There have been extensive studies on the self-exchange of the $Cl^- + CH_3Cl$ reaction by different groups,^{85–89} and the reported free energy barriers are in the range of 26–27 kcal/mol. Our results are in good agreement with those from the literature. The inclusion of the explicit water polarizability increases the barrier by \sim 1.3 kcal/mol (or \sim 5%).

The intramolecular proton transfer reaction of glycine is illustrated in Figure 1. While the neutral form (NF) of the glycine is energetically more stable than the zwitterion (ZW) form in the gas phase by more than 20 kcal/mol (see Figure 5), the ZW is the predominant form in water, which indicates that the water solvent plays a critical role in stabilizing the ZW form. The glycine intramolecular proton transfer reaction has also been widely studied through many different theoretical methods, including the polarizable continuum model (PCM),⁹⁰ the water cluster plus the PCM modeling,^{91–93} the EVB description,^{94,95} the QM/MM treatment,^{96–98} and the CPMD simulation.⁹⁹ While the experimentally measured free energy difference of the form (ZW) and the neutral form (NF) of glycine in aqueous solution is about 7.27 kcal/mol,¹⁰⁰ the reported theoretical values of the free energy difference between the ZW conformer and the NF conformer were in a wide range, from about 4.8 to 11.2 kcal/mol. In this work, we used B3LYP/6–31G(d) for the QM calculations and the TIP3P and SWM4–NDP water models. As shown in Figure 5, by comparing with the results from MP2/aug-cc-pvtz, we find that B3LYP/6–31G(d) is fairly accurate in describing this intramolecule proton reaction in the gas phase. Figure 6 demonstrates that the employment of the polarizable force field has a strong effect on the resulted free energy reaction profiles in the aqueous solution. We obtained a 7.4 kcal/mol transition state barrier and a free energy difference of 4.4 kcal/mol between the ZW and the NF from the B3LYP(6–31G(d))/TIP3P simulation. The corresponding B3LYP(6–31G(d))/SWM4–NDP simulation gives a barrier of 8.9 kcal/mol and a free energy difference of 6.4 kcal/mol. By collecting the data from the reactant region (ZW) defined as $-1.5 \text{ \AA} < rc < -0.8 \text{ \AA}$ and the product region (NF) defined as $0.6 \text{ \AA} < rc < 1.0 \text{ \AA}$, we find the difference of the averaged glycine–water interaction energy between the ZW and NF is 73 kcal/mol from the QM/MM simulation and 83 kcal/mol from the QM/MM-Drude simulation. Apparently the polarizable water model gives a relatively stronger glycine–water interaction for the ZW. As shown in Figure 7, there is no significant difference of the radial distribution functions between the TIP3P and SWM4–NDP water model. However, as illustrated in Figure 8, we observe that the averaged SWM4–NDP water dipoles within the first solvation shell of the N1 atom of glycine in the ZW form are significantly larger than the dipole of TIP3P water (2.35 Deybe). Our results here suggest that the polarizable water model can strongly affect the resulted free energy reaction profiles by influencing the QM/MM interactions without changing the solvation structure.

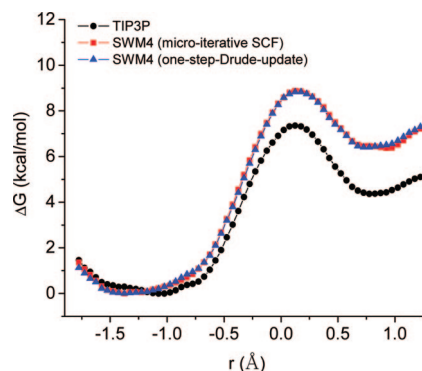
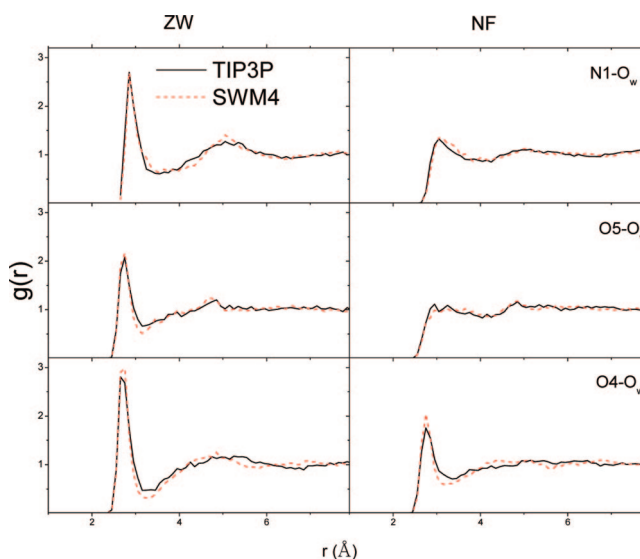
Table 1. Comparison of SCF Steps and Time Ratios between ai-QM/MM and ai-QM/MM-Drude with Different Schemes of Optimizing/Updating the Positions of Drude Particles during MD Simulations^a

| | | ai-QM/MM-Drude | | | | |
|---|------------|----------------|--------------------|------------|-----------------------|----------|
| | | ai-QM/MM | microiterative SCF | direct SCF | one-step-Drude-update | dual SCF |
| Cl ⁻ + CH ₃ Cl (HF 59 basis sets) | SCF steps | 6.2 | 6.1 | 6.1 | 6.1 | 10.4 |
| | time ratio | 1.0 | 2.4 | 2.0 | 1.6 | 3.4 |
| glycine (B3LYP 85 basis sets) | SCF steps | 7.0 | 7.0 | 7.0 | 7.0 | 11.5 |
| | time ratio | 1.0 | 1.7 | 1.5 | 1.25 | 2.0 |
| adenosine (HF 311 basis sets) | SCF steps | 7.0 | 7.0 | 7.0 | 7.0 | 10.7 |
| | time ratio | 1.0 | 1.13 | 1.09 | 1.05 | 1.44 |

^a For calculating the time ratio, we have employed the computational cost of ai-QM/MM calculations as the reference.

**Figure 4.** Potential of mean force for the Cl⁻ + CH₃Cl reaction in TIP3P and in SWM4-NDP obtained using the microiterative SCF scheme and the one-step-Drude-update scheme.**Figure 5.** Energies of the glycine intramolecular proton transfer reaction in gas phase.

All the calculations described above have employed the microiterative SCF scheme so that the Drude positions are fully converged at each MD step. Such simulations are more expensive than the one-step-Drude-update scheme as presented in section II.E. Since the Drude positions are not fully converged in the one-step-Drude-update scheme, one concern is that the Drude particles may exert systematic drag forces on the physical atoms along the MD simulations, which affects the resulted PMF. As a test, we employed the one-step-Drude-update scheme in our ai-QM/MM-Drude MD simulations for the PMF calculations of the two chemical reactions described above. To make sure the Drude particles stay close to the SCF regime, we switched to the microiterative SCF scheme every 100 MD steps. From Figures 4 and 6, we can see that the curves obtained with different

**Figure 6.** Potential of mean force for the glycine intramolecular proton transfer reaction in TIP3P and in SWM4-NDP obtained using the microiterative SCF scheme and the one-step-Drude-update scheme.**Figure 7.** Radial distribution functions g_{N1-Ow} (top), g_{O5-Ow} (middle), and g_{O4-Ow} (bottom) of the glycine in the ZW form (left panel) and the NF form (right panel) solvated in TIP3P and SWM4-NDP waters.

schemes overlap very well with each other, which suggests the promise of the one-step-Drude-update scheme in the QM/MM-Drude MD simulations.

V. Conclusion

In this work, we have presented a detailed description of the methodologies of coupling the ab initio QM methods with the classical Drude oscillator model and applied the ai-QM/MM-Drude approach to the PMF calculations of two

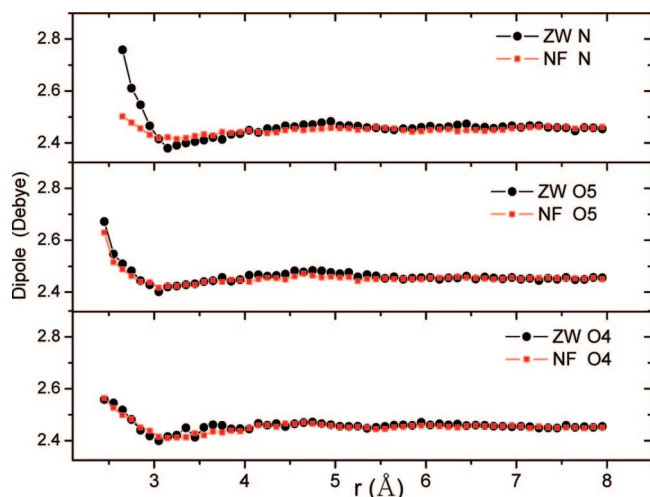


Figure 8. Averaged water dipoles in the ZW form and the NF form of glycine along r_{N1-Ow} , r_{O5-Ow} , and r_{O4-Ow} .

chemical reactions in solution. Besides the dual SCF, direct SCF, and microiterative SCF schemes, we have presented a one-step-Drude-update scheme, in which the Drude positions of MM subsystem are updated only once instead of fully converged during each molecular dynamics simulation step. The resulted ai-QM/MM-Drude MD simulations are found to be highly efficient and yield chemical reaction free energy profiles in quantitative agreement with the corresponding fully converged-Drude-update simulations. In comparison with the corresponding ai-QM/MM calculations, the computational cost overhead for the ai-QM/MM-Drude calculations with efficient implementation schemes is rather insignificant when the QM subsystem consists of tens of atoms, which is typical for most ai-QM/MM applications. The feasibility and applicability of the implemented ai-QM/MM-Drude approach have been demonstrated by performing the potentials of mean force calculations for both the methyl transfer reaction of the methyl chlorine-chlorine ion system and the glycine intramolecular proton transfer reaction in aqueous solution. Compared with the results from ai-QM/MM, the relative effects on the free energy profiles by switching from TIP3P to a polarizable water model for the MM environment are found to be significant for the glycine intramolecular transfer reaction. With the continuing development of polarizable MM force fields and the further improvement in describing QM/MM interactions, the ai-QM/MM-Drude approach should become a more robust approach than the conventional QM/MM approach in modeling chemical reactions in solutions and biological systems.

Acknowledgment. We thank Dr. Shenglong Wang for helpful discussion. This work has been supported by the National Institutes of Health (R01-GM079223) and the National Science Foundation (CHE-CAREER-0448156). We thank NYU-ITS and NCSA for providing computational resources and support.

References

- (1) Warshel, A.; Levitt, M. Theoretic studies of enzymic reactions: dielectric electrostatic and steric stabilization of the carbonium ion in the reaction of lysozyme. *J. Mol. Biol.* **1976**, *103*, 227–249.
- (2) Field, M. J.; Bash, P. A.; Karplus, M. A combined quantum-mechanical and molecular mechanical potential for molecular-dynamics simulations. *J. Comput. Chem.* **1990**, *11*, 700–733.
- (3) Gao, J. L.; Truhlar, D. G. Quantum mechanical methods for enzyme kinetics. *Annu. Rev. Phys. Chem.* **2002**, *53*, 467–505.
- (4) Hammes-schiffer, S. Quantum-classical simulation methods for hydrogen transfer in enzymes: a case study of dihydrofolate reductase. *Curr. Opin. Struct. Biol.* **2004**, *14*, 192–201.
- (5) Garcia-viloca, M.; Gao, J.; Karplus, M.; Truhlar, D. G. How enzymes work: analysis by modern rate theory and computer simulations. *Science* **2004**, *303*, 186–195.
- (6) Friesner, R. A.; Guallar, V. Ab initio quantum chemical and mixed quantum mechanics/molecular mechanics (QM/MM) methods for studying enzymatic catalysis. *Annu. Rev. Phys. Chem.* **2005**, *56*, 389–427.
- (7) Riccardi, D.; Schaefer, P.; Yang, Y.; Yu, H. B.; Ghosh, N.; Prat-Resina, X.; Konig, P.; Li, G. H.; Xu, D. G.; Guo, H.; Elstner, M.; Cui, Q. Development of effective quantum mechanical/molecular mechanical (QM/MM) methods for complex biological processes. *J. Phys. Chem. B* **2006**, *110*, 6458–6469.
- (8) Zhang, Y. Pseudobond ab initio QM/MM approach and its applications to enzyme reactions. *Theor. Chem. Acc.* **2006**, *116*, 43–50.
- (9) Senn, H. M.; Thiel, W. QM/MM studies of enzymes. *Curr. Opin. Chem. Biol.* **2007**, *11*, 182–187.
- (10) Lin, H.; Truhlar, D. G. QM/MM: what have we learned, where are we, and where do we go from here. *Theor. Chem. Acc.* **2007**, *117*, 185–199.
- (11) Shurki, A.; Warshel, A. Structure/function correlations of proteins using mm, qm/mm, and related approaches: methods, concepts, pitfalls, and current progress. *Adv. Protein Chem.* **2003**, *66*, 249–313.
- (12) Yang, W.; Hu, H. Free energies of chemical reactions in solution and in enzymes with ab initio quantum mechanical/molecular mechanics methods. *Annu. Rev. Phys. Chem.* **2008**, *59*, 573–601.
- (13) Singh, U. C.; Kollman, P. A. A combined ab initio quantum mechanical and molecular mechanical method for carrying out simulations on complex molecular systems: applications to the $\text{CH}_3\text{Cl} + \text{Cl}^-$ exchange reaction and gas phase protonation of polyethers. *J. Comput. Chem.* **1986**, *7*, 718–730.
- (14) Stanton, R. V.; Hartsough, D. S.; Merz, K. M. Calculation of Solvation Free Energies Using a Density Functional/Molecular Dynamics Coupled Potential. *J. Phys. Chem.* **1993**, *97*, 11868–11870.
- (15) Yarne, D. A.; Tuckerman, M. E.; Martyna, G. J. A dual length scale method for plane-wave-based, simulation studies of chemical systems modeled using mixed ab initio/empirical force field descriptions. *J. Chem. Phys.* **2001**, *115*, 3531–3539.
- (16) Carloni, P.; Rothlisberger, U.; Parrinello, M. The role and perspective of a initio molecular dynamics in the study of biological systems. *Acc. Chem. Res.* **2002**, *35*, 455–464.
- (17) Rega, N.; Iyengar, S. S.; Voth, G. A.; Schlegel, H. B.; Vreven, T.; Frisch, M. J. Hybrid ab-initio/empirical molecular dynamics: combining the oniom scheme with the atom-

- centered density matrix propagation (admp) approach. *J. Phys. Chem. B* **2004**, *108*, 4210–4220.
- (18) Hu, P.; Wang, S.; Zhang, Y. How do SET-domain protein lysine methyltransferases achieve the methylation state specificity? Revisited by ab initio QM/MM molecular dynamics simulations. *J. Am. Chem. Soc.* **2008**, *130*, 3806–3813.
- (19) Wang, S.; Hu, P.; Zhang, Y. Ab initio quantum mechanical/molecular mechanical molecular dynamics simulation of enzyme catalysis: The case of histone lysine methyltransferase SET7/9. *J. Phys. Chem. B* **2007**, *111*, 3758–3764.
- (20) Thompson, M. A.; Schenter, G. K. Excited states of the bacteriochlorophyll b dimmer of *Rhodospseudomonas viridis*: A QM/MM study of the photosynthetic reaction center that includes MM polarization. *J. Phys. Chem.* **1995**, *99*, 6374–6386.
- (21) Thompson, M. A. Qm/mmpol: a consistent model for solute/solvent polarization. application to the aqueous solvation and spectroscopy of formaldehyde, acetaldehyde, and acetone. *J. Phys. Chem.* **1996**, *100*, 14492–14507.
- (22) Bakowies, D.; Thiel, W. Hybrid Models for Combined Quantum Mechanical and Molecular Mechanical Approaches. *J. Phys. Chem.* **1996**, *100*, 10580–10594.
- (23) Gao, J. L. Energy components of aqueous solution: insight from hybrid qm/mm simulations using a polarizable solvent model. *J. Comput. Chem.* **1997**, *18*, 1061–1071.
- (24) Aida, M.; Yamataka, H.; Dupuis, M. Critical assessment of the hybrid QM/MM-pol-vib approach: Small water clusters using polarizable flexible water potentials. *Int. J. Quantum Chem.* **2000**, *77*, 199–210.
- (25) Houjou, H.; Inoue, Y.; Sakurai, M. Study of the opsin shift of bacteriorhodopsin: insight from qm/mm calculations with electronic polarization effects of the protein environment. *J. Phys. Chem. B* **2001**, *105*, 867–879.
- (26) Dupuis, M.; Aida, M.; Kawashima, Y.; Hirao, K. A polarizable mixed hamiltonian model of electronic structure for micro-solvated excited states. i. energy and gradients formulation and application to formaldehyde (1A_2). *J. Chem. Phys.* **2002**, *117*, 1242–1255.
- (27) Dupuis, M.; Kawashima, Y.; Hirao, K. A polarizable mixed Hamiltonian model of electronic structure for solvated excited states. II. Application to the blue shift of the H_2CO ($^1\pi^* \leftarrow n$) excitation in water. *J. Chem. Phys.* **2002**, *117*, 1256–1268.
- (28) Kongsted, J.; Osted, A.; Mikkelsen, K. V.; Christiansen, O. Coupled cluster/molecular mechanics method: Implementation and application to liquid water. *J. Phys. Chem. A* **2003**, *107*, 2578–2588.
- (29) Jensen, L.; Duijnen, P. T.v.; Snijders, J. G. A discrete solvent reaction field model within density functional theory. *J. Chem. Phys.* **2003**, *118*, 514–521.
- (30) Illingworth, C. J. R.; Gooding, S. R.; Winn, P. J.; Jones, G. A.; Ferenczy, G. G.; Reynolds, C. A. Classical polarization in hybrid QM/MM methods. *J. Phys. Chem. A* **2006**, *110*, 6487–6497.
- (31) Nielsen, C. B.; Christiansen, O.; Mikkelsen, K. V.; Kongsted, J. Density functional self-consistent quantum mechanics/molecular mechanics theory for linear and nonlinear molecular properties: Applications to solvated water and formaldehyde. *J. Chem. Phys.* **2007**, *126* (15), 154112–154118.
- (32) Lin, Y. L.; Gao, J. L. Solvatochromic shifts of the $n \rightarrow \pi^*$ transition of acetone from steam vapor to ambient aqueous solution: A combined configuration interaction QM/MM simulation study incorporating solvent polarization. *J. Chem. Theory Comput.* **2007**, *3*, 1484–1493.
- (33) Bryce, R. A.; Buesnel, R.; Hillier, I. H.; Burton, N. A. A solvation model using a hybrid quantum mechanical/molecular mechanical potential with fluctuating solvent charges. *Chem. Phys. Lett.* **1997**, *279*, 367–371.
- (34) Field, M. J. Hybrid quantum mechanical molecular mechanical fluctuating charge models for condensed phase simulations. *Mol. Phys.* **1997**, *91*, 835–845.
- (35) Geerke, D. P.; Thiel, S.; Thiel, W.; van Gunsteren, W. F. Combined QM/MM molecular dynamics study on a condensed-phase S_N2 reaction at nitrogen: The effect of explicitly including solvent polarization. *J. Chem. Theory Comput.* **2007**, *3*, 1499–1509.
- (36) Washel, A.; Kato, M.; Pislakov, A. V. Polarizable Force Fields: History, Test Cases, and Prospects. *J. Chem. Theory Comput.* **2007**, *3*, 2034–2045.
- (37) Zhang, Y.; Lin, H.; Truhlar, D. G. Self-consistent polarization of the boundary in the redistributed charge and dipole scheme for combined quantum-mechanical and molecular-mechanical calculations. *J. Chem. Theory Comput.* **2007**, *3*, 1378–1398.
- (38) Hannachi, Y.; Angyan, J. G. The role of induction forces in infrared matrix shifts - quantum chemical calculations with reaction field model hamiltonian. *THEOCHEM - J. Mol. Struct.* **1991**, *78*, 97–110.
- (39) Jansen, G.; Colonna, F.; Angyan, J. G. Mixed quantum-classical calculations on the water molecule in liquid phase: Influence of a polarizable environment on electronic properties. *Int. J. Quantum Chem.* **1996**, *58*, 251–265.
- (40) Thole, B. T.; Vanduijnen, P. T. On the quantum-mechanical treatment of solvent effects. *Theor. Chim. Acta* **1980**, *55* (4), 307–318.
- (41) van Duijnen, P. T.; Grozema, F.; Swart, M. Some applications of the direct reaction field approach. *THEOCHEM - J. Mol. Struct.* **1999**, *464*, 191–198.
- (42) Rick, S. W.; Stuart, S. J. Potentials and algorithms for incorporating polarizability in computer simulations. In *Review in Computational Chemistry*; VCH: New York, 2002; Vol. 18, pp 89–146.
- (43) Ponder, J. W.; Case, D. A. Force fields for protein simulations. *Adv. Protein Chem.* **2003**, *66*, 27–85.
- (44) Cieplak, P.; Caldwell, J.; Kollman, P. Molecular mechanical models for organic and biological systems going beyond the atom centered two body additive approximation: aqueous solution free energies of methanol and n-methyl acetamide, nucleic acid base, and amide hydrogen bonding and chloroform/water partition coefficients of the nucleic acid bases. *J. Comput. Chem.* **2001**, *22*, 1048–1057.
- (45) Kaminski, G. A.; Stern, H. A.; Berne, B. J.; Friesner, R. A.; Cao, Y. X. X.; Murphy, R. B.; Zhou, R. H.; Halgren, T. A. Development of a polarizable force field for proteins via ab initio quantum chemistry: first generation model and gas phase tests. *J. Comput. Chem.* **2002**, *23*, 1515–1531.
- (46) Ren, P. Y.; Ponder, J. W. Polarizable atomic multipole water model for molecular mechanics simulation. *J. Phys. Chem. B* **2003**, *107*, 5933–5947.
- (47) Kaminski, G. A.; Stern, H. A.; Berne, B. J.; Friesner, R. A. Development of an accurate and robust polarizable molecular

- mechanics force field from ab initio quantum chemistry. *J. Phys. Chem. A* **2004**, *108*, 621–627.
- (48) Rappe, A. K.; Goddard, W. A. Charge equilibration for molecular-dynamics simulations. *J. Phys. Chem.* **1991**, *95*, 3358–3363.
- (49) Rick, S. W.; Stuart, S. J.; Berne, B. J. Dynamical fluctuating charge force-fields - application to liquid water. *J. Chem. Phys.* **1994**, *101*, 6141–6156.
- (50) York, D. M.; Yang, W. T. A chemical potential equalization method for molecular simulations. *J. Chem. Phys.* **1996**, *104*, 159–172.
- (51) Patel, S.; Brooks, C. L. Charmm fluctuating charge force field for proteins: i parameterization and application to bulk organic liquid simulations. *J. Comput. Chem.* **2004**, *25*, 1–15.
- (52) Drude, P. *The Theory of Optics*; Longmans, Green, and Co.: New York, 1902.
- (53) Born, M.; Huang, K. *Dynamic Theory of Crystal Lattices*; Oxford University Press: Oxford, U.K., 1954.
- (54) Straatsma, T. P.; McCammon, J. A. Molecular Dynamics Simulations with Interaction Potentials Including Polarization. Development of a Noniterative Method and Application to Water. *Mol. Simul.* **1990**, *5*, 181–192.
- (55) van Maaren, P. J.; van der Spoel, D. Molecular dynamics simulations of water with novel shell-model potentials. *J. Phys. Chem. B* **2001**, *105*, 2618–2626.
- (56) Yu, H. B.; Hansson, T.; van Gunsteren, W. F. Development of a simple, self-consistent polarizable model for liquid water. *J. Chem. Phys.* **2003**, *118*, 221–234.
- (57) Lamoureux, G.; Roux, B. Modeling induced polarization with classical drude oscillators: theory and molecular dynamics simulation algorithm. *J. Chem. Phys.* **2003**, *119*, 3025–3039.
- (58) Yu, H. B.; van Gunsteren, W. F. Charge-on-spring polarizable water models revisited: From water clusters to liquid water to ice. *J. Chem. Phys.* **2004**, *121*, 9549–9564.
- (59) Yu, H. B.; van Gunsteren, W. F. Accounting for polarization in molecular simulation. *Comput. Phys. Commun.* **2005**, *172*, 69–85.
- (60) Anisimov, V. M.; Lamoureux, G.; Vorobyov, I. V.; Huang, N.; Roux, B.; MacKerell, A. D. Determination of electrostatic parameters for a polarizable force field based on the classical Drude oscillator. *J. Chem. Theory Comput.* **2005**, *1*, 153–168.
- (61) Vorobyov, I. V.; Anisimov, V. M.; MacKerell, A. D. Polarizable empirical force field for alkanes based on the classical drude oscillator model. *J. Phys. Chem. B* **2005**, *109*, 18988–18999.
- (62) Harder, E.; Anisimov, V. M.; Vorobyov, I. V.; Lopes, P. E. M.; Noskov, S. Y.; MacKerell, A. D.; Roux, B. Atomic level anisotropy in the electrostatic modeling of lone pairs for a polarizable force field based on the classical Drude oscillator. *J. Chem. Theory Comput.* **2006**, *2*, 1587–1597.
- (63) Geerke, D. P.; van Gunsteren, W. F. Calculation of the free energy of polarization: Quantifying the effect of explicitly treating electronic polarization on the transferability of force-field parameters. *J. Phys. Chem. B* **2007**, *111*, 6425–6436.
- (64) Lamoureux, G.; MacKerell, A. D.; Roux, B. A simple polarizable model of water based on classical Drude oscillators. *J. Chem. Phys.* **2003**, *119*, 5185–5197.
- (65) Lamoureux, G.; Harder, E.; Vorobyov, I. V.; Roux, B.; MacKerell, A. D. A polarizable model of water for molecular dynamics simulations of biomolecules. *Chem. Phys. Lett.* **2006**, *418*, 245–249.
- (66) Geerke, D. P.; van Gunsteren, W. On the Calculation of Atomic Forces in Classical Simulation Using the Charge-on-Spring Method To Explicitly Treat Electronic Polarization. *J. Chem. Theory Comput.* **2007**, *3*, 2128–2137.
- (67) Sprik, M.; Klein, M. L. A polarizable model for water using distributed charge sites. *J. Chem. Phys.* **1988**, *89*, 7556–7560.
- (68) Lamoureux, G.; Roux, B. Modeling induced polarization with classical Drude oscillators: Theory and molecular dynamics simulation algorithm. *J. Chem. Phys.* **2003**, *119*, 3025–3039.
- (69) Kolafa, J. Numerical integration of equations of motion with a self-consistent field given by an implicit equation. *Mol. Simul.* **1996**, *18*, 193–212.
- (70) Kolafa, J. Time-reversible always stable predictor-corrector method for molecular dynamics of polarizable molecules. *J. Comput. Chem.* **2004**, *25*, 335–342.
- (71) Niklasson, A. M. N.; Tymczak, C. J.; Challacombe, M. Time-reversible Born-Oppenheimer molecular dynamics. *Phys. Rev. Lett.* **2006**, *97*.
- (72) Niklasson, A. M. N.; Tymczak, C. J.; Challacombe, M. Time-reversible ab initio molecular dynamics. *J. Chem. Phys.* **2007**, *126*.
- (73) Jorgensen, W. L.; Chandrasekhar, J.; Madura, J. D.; Impey, R. W.; Klein, M. L. Comparison of Simple Potential Functions for Simulating Liquid Water. *J. Chem. Phys.* **1983**, *79*, 926–935.
- (74) Frisch, M. J.; Trucks, G. W.; Schlegel, H. B.; Scuseria, G. E.; Robb, M. A.; Cheeseman, J. R.; Montgomery, J. A., Jr.; Vreven, T.; Kudin, K. N.; Burant, J. C.; Millam, J. M.; Iyengar, S. S.; Tomasi, J.; Barone, V.; Mennucci, B.; Cossi, M.; Scalmani, G.; Rega, N.; Petersson, G. A.; Nakatsuji, H.; Hada, M.; Ehara, M.; Toyota, K.; Fukuda, R.; Hasegawa, J.; Ishida, M.; Nakajima, T.; Honda, Y.; Kitao, O.; Nakai, H.; Klene, M.; Li, X.; Knox, J. E.; Hratchian, H. P.; Cross, J. B.; Adamo, C.; Jaramillo, J.; Gomperts, R.; Stratmann, R. E.; Yazyev, O.; Austin, A. J.; Cammi, R.; Pomelli, C.; Ochterski, J. W.; Ayala, P. Y.; Morokuma, K.; Voth, G. A.; Salvador, P.; Dannenberg, J. J.; Zakrzewski, V. G.; Dapprich, S.; Daniels, A. D.; Strain, M. C.; Farkas, O.; Malick, D. K.; Rabuck, A. D.; Raghavachari, K.; Foresman, J. B.; Ortiz, J. V.; Cui, Q.; Baboul, A. G.; Clifford, S.; Cioslowski, J.; Stefanov, B. B.; Liu, G.; Liashenko, A.; Piskorz, P.; Komaromi, I.; Martin, R. L.; Fox, D. J.; Keith, T.; Al-Laham, M. A.; Peng, C. Y.; Nanayakkara, A.; Challacombe, M.; Gill, P. M. W.; Johnson, B.; Chen, W.; Wong, M. W.; Gonzalez, C.; Pople, J. A. *Gaussian 03*, Revision D.01; Gaussian, Inc.: Wallingford, CT, 2004.
- (75) Ponder, J. W. TINKER, Software Tools for Molecular Design, Version 4.2. The most updated version for the TINKER program can be obtained from J. W. Ponder's World Wide Web at <http://dasher.wustl.edu/tinker>, June 2004.
- (76) Ryckaert, J.-P.; Ciccotti, G.; Berendsen, H. J. C. Numerical Integration of the Cartesian Equations of Motion of a System with Constraints: Molecular Dynamics of n-Alkanes. *J. Comput. Phys.* **1977**, *23*, 327–341.
- (77) Andersen, H. C. RATTLE - A velocity version of the shake algorithm for molecular-dynamics calculations. *J. Comput. Phys.* **1983**, *52*, 24–34.

- (78) Berendsen, H. J. C.; Postma, J. P. M.; Gunsteren, W. F. V.; DiNola, A.; Haak, J. R. Molecular dynamics with coupling to an external bath. *J. Chem. Phys.* **1984**, *81*, 684–690.
- (79) Ferrenberg, A. M.; Swendsen, R. H. Optimized monte-carlo data-analysis. *Phys. Rev. Lett.* **1989**, *63*, 1195–1198.
- (80) Kumar, S.; Bouzida, D.; Swendsen, R. H.; Kollman, P. A.; Rosenberg, J. M. The weighted histogram analysis method for free-energy calculations on biomolecules. 1. the method. *J. Comput. Chem.* **1992**, *13*, 1011–1021.
- (81) Cornell, W. D.; Cieplak, P.; Bayly, C. I.; Gould, I. R.; Merz, K. M.; Ferguson, D. M.; Spellmeyer, D. C.; Fox, T.; Caldwell, J. W.; Kollman, P. A. A Second Generation Force Field for the Simulation of Proteins, Nucleic Acids and Organic Molecules. *J. Am. Chem. Soc.* **1995**, *117*, 5179–5197.
- (82) Freindorf, M.; Gao, J. L. Optimization of the lennard-jones parameters for a combined ab initio quantum mechanical and molecular mechanical potential using the 3–21g basis set. *J. Comput. Chem.* **1996**, *17*, 386–395.
- (83) Riccardi, D.; Li, G. H.; Cui, Q. Importance of van der waals interactions in qm/mm simulations. *J. Phys. Chem. B* **2004**, *108*, 6467–6478.
- (84) Freindorf, M.; Shao, Y. H.; Furlani, T. R.; Kong, J. Lennard-Jones parameters for the combined QM/MM method using the B3LYP/6–31+G*/AMBER potential. *J. Comput. Chem.* **2005**, *26* (12), 1270–1278.
- (85) Chandrasekhar, J.; Smith, S. F.; Jorgensen, W. L. Theoretical examination of S_N2 reaction involving chloride ion and methyl chloride in the gas phase and aqueous solution. *J. Am. Chem. Soc.* **1985**, *107*, 154–162.
- (86) Hwang, J. K.; King, G.; Creighton, S.; Warshel, A. Simulation of free-energy relationships and dynamics of $sn2$ reactions in aqueous-solution. *J. Am. Chem. Soc.* **1988**, *110*, 5297–5311.
- (87) Jorgensen, W. L. Free Energy Calculations: A Breakthrough for Modeling Organic Chemistry in Solution. *Acc. Chem. Res.* **1989**, *22*, 184–189.
- (88) Bash, P. A.; Field, M. J.; Karplus, M. Free-energy perturbation method for chemical-reactions in the condensed phase - a dynamical-approach based on a combined quantum and molecular mechanics potential. *J. Am. Chem. Soc.* **1987**, *109*, 8092–8094.
- (89) Mo, Y. R.; Gao, J. L. Ab initio QM/MM simulations with a molecular orbital-valence bond (MOVb) method: Application to an S_N2 reaction in water. *J. Comput. Chem.* **2000**, *21*, 1458–1469.
- (90) Tunon, I.; Silla, E.; Ruiz-Lopez, M. F. On the tautomerization process of glycine in aqueous solution. *Chem. Phys. Lett.* **2000**, *321*, 433–437.
- (91) Fernandez-Ramos, A.; Smedarchina, Z.; Siebrand, W.; Zgierski, M. Z. A direct-dynamics study of the zwitterion-to-neutral interconversion of glycine in aqueous solution. *J. Chem. Phys.* **2000**, *113*, 9714–9721.
- (92) Bandyopadhyay, P.; Gordon, M. S.; Mennucci, B.; Tomasi, J. An integrated effective fragment-polarizable continuum approach to solvation: Theory and application to glycine. *J. Chem. Phys.* **2002**, *116*, 5023–5032.
- (93) Aikens, C. M.; Gordon, M. S. Incremental solvation of nonionized and zwitterionic glycine. *J. Am. Chem. Soc.* **2006**, *128*, 12835–12850.
- (94) Okuyama-Yoshida, N.; Nagaoka, M.; Yamabe, T. Potential energy function for intramolecular proton transfer reaction of glycine in aqueous solution. *J. Phys. Chem. A* **1998**, *102*, 285–292.
- (95) Nagaoka, M.; Okuyama-Yoshida, N.; Yamabe, T. Origin of the transition state on the free energy surface: Intramolecular proton transfer reaction of glycine in aqueous solution. *J. Phys. Chem. A* **1998**, *102*, 8202–8208.
- (96) Tunon, I.; Silla, E.; Millot, C.; Martins-Costa, M. T. C.; Ruiz-Lopez, M. F. Intramolecular proton transfer of glycine in aqueous solution using quantum mechanics-molecular mechanics simulations. *J. Phys. Chem. A* **1998**, *102*, 8673–8678.
- (97) Shoeib, T.; Ruggiero, G. D.; Siu, K. W. M.; Hopkinson, A. C.; Williams, I. H. A hybrid quantum mechanical molecular mechanical method: Application to hydration free energy calculations. *J. Chem. Phys.* **2002**, *117*, 2762–2770.
- (98) Takahashi, H.; Kawashima, Y.; Nitta, T.; Matubayasi, N. A novel quantum mechanical/molecular mechanical approach to the free energy calculation for isomerization of glycine in aqueous solution. *J. Chem. Phys.* **2005**, *123*.
- (99) Leung, K.; Rempe, S. B. Ab initio molecular dynamics study of glycine intramolecular proton transfer in water. *J. Chem. Phys.* **2005**, *122*.
- (100) Wada, G.; Tamura, E.; Okina, M.; Nakamura, M. On the ratio of zwitterion form to uncharged form of glycine at equilibrium in various aqueous-media. *Bull. Chem. Soc. Jpn.* **1982**, *55*, 3064–3067.

CT800116E